E1-2006-54

S. R. Hashemi-Nezhad[1], I. V. Zhuk[2], A. S. Potapenko[2],
M. I. Krivopustov

CALIBRATION OF TRACK DETECTORS FOR FISSION RATE DETERMINATION: AN EXPERIMENTAL AND THEORETICAL STUDY

[1] School of Physics, University of Sydney, Australia
E-mail: reza@physics.usyd.edu.au
[2] Joint Institute of Power and Nuclear Research (Sosny NASB),
220109 Minsk, Belarus

Хашеми-Нежад С. Р. и др. E1-2006-54
Калибровка твердотельных трековых детекторов ядер для определения скорости деления: экспериментальное и теоретическое изучение

Для определения скорости деления в делящихся материалах при помощи твердотельных трековых детекторов (слюда, лавсан и стекло) экспериментально найден и рассчитан методом Монте-Карло калибровочный фактор w. Показано, что калибровочный фактор w, определенный в полях нейтронов низких энергий, может использоваться для нахождения скорости деления в нейтронных полях с неизвестными характеристиками (энергия и угловое распределение). Это утверждение справедливо, если для вычисления калибровочного фактора w и последующего его применения используется среднее значение плотности треков осколков деления, которое определяется с помощью трековых детекторов, расположенных по обе стороны фольги из делящегося вещества.

Работа выполнена в Лаборатории высоких энергий им. В. И. Векслера и А. М. Балдина ОИЯИ.

Сообщение Объединенного института ядерных исследований. Дубна, 2006

Hashemi-Nezhad S. R. et al. E1-2006-54
Calibration of Track Detectors for Fission Rate Determination: an Experimental and Theoretical Study

The calibration factor w, for the determination of fission rate in fissionable materials using the track detectors (mica, Lavsan, and soda glass) was studied experimentally and by the Monte Carlo method. It is shown that w obtained via low-energy particle induced fission, can be used for the determination of fission rate in a particle (neutron) field of unknown characteristics (energy and angular distribution) if in the determination of w and in its subsequent use the mean density of the tracks in the track detectors on both sides of the fission foil is used.

The investigation has been performed at the Veksler and Baldin Laboratory of High Energies, JINR.

Communication of the Joint Institute for Nuclear Research. Dubna, 2006

1. INTRODUCTION

Determination of fission rate in a sample containing fissionable nuclei is important in a number of areas such as neutron physics, reactor physics and engineering, as well as fission track dating. The fission process may occur as a result of the irradiation of a sample with fission inducing particles or it may happen spontaneously. Solid state nuclear track detectors [1] provide one of the best tools for such studies:

1) They provide a permanent record of the fission events for multiple analyses.

2) The sample-detector assembly can be made as small as possible and, therefore, induces minimum perturbation in the neutron field being investigated.

3) Because of their small sizes, these detectors can be introduced almost in any location within a complicated setup, for example, inside the fuel assembly of a reactor, etc.

4) With a correct choice of the detector material one can record only fission fragments and avoid the registration of other particles that may be present in the radiation field (such as β's, γ's, and light ions).

For a given track detector a calibration factor can be produced by exposing it to fission fragments from a known fissionable material in a very well defined neutron field. Then one can relate the number of fission tracks and fission events in the sample (and not to the number of the projectiles). Such a calibration factor can be used to obtain the fission rate and thus the amount of the fissionable material in a sample with unknown fissionable material content when it is exposed to a particle field of known flux. Or it may be used to obtain particle flux if a sample with a known type and amount of fissionable material is used. The question arising is: does this calibration factor applicable to other neutron fields, with characteristics different than that used in its determination? Effects of the energy spectrum and orientation of the fission inducing particles on the calibration factor will be examined in this paper.

Although our experiments were done using neutron irradiation the resulting experimental and theoretical findings are not restricted to neutrons alone (especially those of the Monte Carlo calculations) and are equally valid for any type of particle that can induce fission in the system of interest, such as protons, deuterons, pions, etc.

2. THEORETICAL BACKGROUND

Calibration Factor for Randomly Oriented Fission Fragments. The fission track density in the external surface of a thick track recording material (detector), such as natural mica, apatite, etc., within which fission events are induced by external irradiation, e. g., by neutrons, is given by [1]

$$\rho = \frac{1}{2} N_f R \cos^2 \theta_c, \tag{1}$$

where ρ is the fission track density at the detector surface (tracks/cm^2), N_f is the number of fission events per unit volume of the detector, R is the mean range of the fission fragments within the foil (environment within which fission takes place) and θ_c is the critical etching angle (smallest dip angle of the fragments with the track detector surface, which can result in etched track [1]). The θ_c is defined as sin $\theta_c = V_\perp / V_T$, where $V_\perp$ is the bulk-etch rate of the detector material in direction normal to the detector surface and V_T is the etch-rate along the damage trial. A sample (foil) will be referred to as a thick sample, if its thickness is more than the mean range of the fission fragments in the foil material. In driving Eq. (1), it is assumed that fission events take place in random locations within the sample and fission fragments have random orientations, i. e., there is no angular anisotropy on the emission directions of the fission fragments.

Equation (1) is valid also in the case when a track detector is placed in close contact with a thick fissionable material (e. g. uranium). The N_f is given by

$$N_f = N_v t \int_0^\infty \sigma_f(E) \varphi(E) dE, \tag{2}$$

where N_v is the number of fissionable nuclei per unit volume of the foil, $\sigma_f(E)$ and $\phi(E)$ are the energy-dependent fission cross section and projectile flux, respectively, and t is the irradiation time.

A more general and elegant representation of the track density at external surface of a foil (track detector containing fissionable nuclei) or in a track detector in close contact with such a foil at different foil thicknesses is given by the following equation [2]:

$$\rho = n \mu \varepsilon d N_v t \int_0^\infty \sigma_f(E) \phi(E) dE, \tag{3}$$

where n is number of the fragments emitted per fission, d is the thickness of the foil, ε is an efficiency factor which includes the critical angle effect, as well as the limitations imposed by the minimum detectable track size and track observation

conditions (as will be discussed later in this paper), and μ accounts for different foil thicknesses and is given by the following relations:

$$\mu = \begin{cases} \frac{1}{2}\left(1 - \frac{d}{2R}\right) & \text{for} \quad d < R, \\ \frac{1}{4} & \text{for} \quad d = R, \\ \frac{1}{4}\frac{R}{d} & \text{for} \quad d > R. \end{cases} \tag{4}$$

In Eqs. (2) and (3) the quantity $t\int\limits_0^\infty \sigma_f(E)\phi(E)dE$ gives the fission per atom of the fissionable nuclei in the foil during the irradiation time t. We define a calibration factor w as

$$w = n\mu\varepsilon dN_v. \tag{5}$$

For example, for a thick ($d > R$) uranium foil we have $w = 2.408 \cdot 10^{22} R\varepsilon$ in units of «track $\cdot$ cm^{-2} $\cdot$ fission^{-1}» or «track$\cdot$ cm^{-2} $\cdot$ neutron^{-1}». Alternatively, w may be expressed as $w = 2.408{\cdot}10^{-2} R\varepsilon$ in units of track $\cdot$ neutron^{-1} $\cdot$ b^{-1} if the cross section is expressed in units of barns rather than in cm^2. This definition of the w implies that if fission track density ρ is measured in a sample, then the ratio of ρ/w represents the number of fissions per atom of the fissionable nuclei in the foil during the irradiation. The w may also be represented per primary incident particle if fission events are induced by secondary particles like in the case of the spallation neutron sources (see, [3, 4]). Experimental and theoretical determinations of the w for different track recording materials under different irradiation conditions are the other aims of this paper.

3. EXPERIMENTAL

Metallic foils of natural uranium and uranium foils enriched with 3.0; 6.5 and 90% ^{235}U were used as fissionable materials. These foils had a diameter of 7 mm and thickness $\sim$ 0.1 mm ($d > R$) and were manufactured by cold rolling and vacuum annealing of the material. The U foils were placed in close contact between two track detector sheets. In our experiments we used four nuclear track recording materials:

1) Natural muscovite mica.

2) Synthetic mica (Fluorophlogopite).

3) Lavsan plastic foil [polyethylene terephthalate; PET (-CO-C_6H_5-CO-O-CH_2-CH_2-O)$_n$].

4) Soda glass (microscope cover glass).

The sample irradiations were performed at two neutron energies. The thermal neutron irradiations were carried out in the thermal column of the F-1 reactor at

the Russian Science Centre «Kurchatov Institute» (Moscow, Russia). Irradiations with 14.7 MeV neutrons were performed at the Russian Special Primary Standard for Units at the «VNIIFTRI» Institute (Mendeleevo, Moscow Region, Russia). For these 14.7 MeV neutron irradiations, the direction of the neutrons was orthogonal to the surface of the detector-foil assembly.

The physical parameters and etching conditions for different detectors are given in Table 1. Track counting was performed manually using photomicrographs obtained via an optical microscope. The track densities were in the range of $5 \cdot 10^4$ – $1 \cdot 10^6$ (tracks $\cdot$ cm^{-2}) and overall magnification of 100X–500X was used (depending on the track density).

Table 1. The physical parameters and etching conditions for different track detectors used in the experiments

Type of SSNTD and its thickness	Etching solution and concentration	Etching temperature, T, °C	Etching time, min
Lavsan (Polyethylene terephthalate); $d = 0.17$ mm	NaOH (10.4N) Density = 1.22 g cm^{-3}	60	30–180
Natural mica, $d = 0.05$ mm	HF, 20%	60	30–120
Artificial mica (Fluorophlogopite) $d = 0.03$ mm	HF, 7%	60	10–40
Soda glass (microscope cover glass) $d = 0.1$ mm	HF, 2%	20	10–60

The calibration factor for thermal and 14.7 MeV neutrons can be calculated from the modified version of Eq. (3), i. e., $\rho = w\phi\sigma$, where ϕ and σ are the neutron flux and fission cross section at these neutron energies.

The parameters and corrections used in the experimental determination of the w and the possible sources of errors are given in the following:

1) The error in density of neutron fluxes in standard neutron fields did not exceed 2% (2σ).

2) Correction factor ξ, for the perturbation of the neutron field caused by the presence of our samples and self-shielding of the neutron flux by the fission foil and the detector, was determined using the following relations [5]:

$$\xi = GL, \quad \text{where} \quad G = \frac{\bar{\varphi}_V}{\bar{\varphi}_S} \quad \text{and} \quad L = \frac{\bar{\varphi}_S}{\bar{\varphi}_0}, \tag{6}$$

where the function G takes into account the self-shielding of neutron flux by the sample and is defined as the ratio of average neutron flux through the volume ($\bar{\varphi}_V$) to the average flux over the surface of the foil ($\bar{\varphi}_S$). The function L takes into account the outer perturbation of neutron field and is determined as the ratio of the average surface flux ($\bar{\varphi}_S$) to the unperturbed flux (φ_0).

As an example, the value of the correction factor ξ for natural uranium-detector sandwich in the thermal neutron field was 0.997 ± 0.002. The correction factor ξ for the standard neutron field with energy 14.7 MeV was practically equal to unity.

3) For ^{235}U at the thermal and 14.7 MeV neutron energies, fission cross sections of 582.6($\pm$0.19%) b [6] and 2.085($\pm$1.2%) b [7], respectively, were used.

4) A ratio of fission cross sections of ^{238}U and ^{235}U at neutron energy of 14.7 MeV, $\left(\sigma_f^{^{238}\mathrm{U}}/\sigma_f^{^{235}\mathrm{U}}\right)_{14.7\,\mathrm{MeV}} = 0.587(\pm 1.1\%)$, [8] was used.

5) Error in track density measurements was less than 2%.

The experimental w values for different types of the thick metallic uranium foils and for four types of the track detectors are given in Table 2. All w values are the mean of those obtained for the track detectors in contact with both surfaces of the relevant fission foil.

Table 2. The experimentally determined calibration factors w in units of (10^{19}track cm^{-2} neutron^{-1}) for different types of track detectors in thermal and 14.7 MeV neutron fields

Type of SSNTD and its thickness	Calibration factor w					**Average**
	Type of the neutron field	Natural U thick metallic foil	3% ^{235}U thick metallic foil	6.5% ^{235}U thick metallic foil	90% ^{235}U thick metallic foil	
Lavsan Polyethylene terephthalate; $d = 0.17$ mm	Thermal	1.21$\pm$0.04	1.16$\pm$0.04	1.15$\pm$0.04	NA*	1.18$\pm$0.04
	14.7 MeV	1.20$\pm$0.04	NA	NA	1.18$\pm$0.04	
Natural mica, $d = 0.05$ mm	Thermal	1.08$\pm$0.04	1.11$\pm$0.04	1.05$\pm$0.04	NA*	1.07$\pm$0.04
	14.7 MeV	1.03$\pm$0.04	NA	NA	1.10$\pm$0.04	
Artificial mica (Fluoro-phlogopite) $d = 0.03$ mm	Thermal	0.95$\pm$0.04	0.97$\pm$0.03	1.02$\pm$0.03	NA*	0.99$\pm$0.03
	14.7 MeV	0.96$\pm$0.03	NA	NA	1.03$\pm$0.04	
Soda glass (microscope cover glass) $d = 0.1$ mm	Thermal	0.61$\pm$0.03	0.60$\pm$0.03	0.57$\pm$0.02	NA*	0.59$\pm$0.02
	14.7 MeV	NA**	NA**	NA**	NA**	

*Very strong self-shielding of neutron flux by the fission foil.

** We didn't use the microscope cover glass for measurements in fast neutron fields.

4. MONTE CARLO SIMULATIONS

We used Monte Carlo (MC) method for detailed studies of the calibration factor w for different foil-detector systems. Figure 1 shows the schematic view of the foil-detector assembly used in the calculations and experiments.

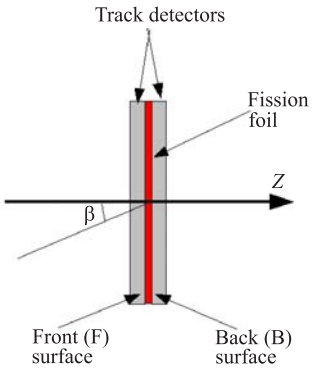

Fig. 1. The schematic view of the foil-detector assembly

A MC code was written to calculate the w at different conditions. In the following, the symbols $w_{\rm B}$ and $w_{\rm F}$ will be used to specify the calibration factors of the back and front detectors (Fig. 1), respectively, and $w_{\rm m}$ will represent the mean value of $w_{\rm B}$ and $w_{\rm F}$ [$w_{\rm m} = (w_{\rm B} + w_{\rm F})/2$]. In this code following assumptions were made.

1) It was assumed that $^{138}_{53}$I and $^{95}_{39}$Y represent the median-heavy and median-light fission fragments of uranium, respectively [9].

2) It was assumed that the *mean range* of the fission fragments does not change significantly with incident neutron energy [10].

3) It was assumed that mean total kinetic energy of the fission fragments is 169 MeV [11, 12].

4) The energy range relations for fragments in the U foil and external detector materials were calculated using the SRIM2003 code [13].

5) It was assumed that fission events take place in random locations within the foil volume. This assumption is justified because of the small size of the uranium foil (diameter of 7 mm and thickness of 100 μm).

6) For every detector a critical dip angle θ_c was used, below which the fission fragment tracks cannot be revealed by chemical etching.

7) It was assumed that there is a minimum track size below which the etched tracks will not be identified as tracks (because of the microscope resolution and observational limitations), and therefore are not counted.

8) Calculations were performed for N_c fission events so that a statistical uncertainty better than 1 % was achieved.

4.1. Comparison of MC Results with Theoretical Expectations. Two tests were applied to examine the integrity of the MC code. First, it was run for the cases of spontaneous fission within U foil (or for a U foil containing ^{235}U irradiated with thermal neutrons). In these calculations θ_c was set to zero and detection restriction was not imposed. Figure 2 shows variations of the $w_{\rm m}$ with foil thickness d. As expected the plateau value of the w is reached when the foil thickness exceeds the mean range of the fission fragments in the uranium ($R =$ 5.41 μm).

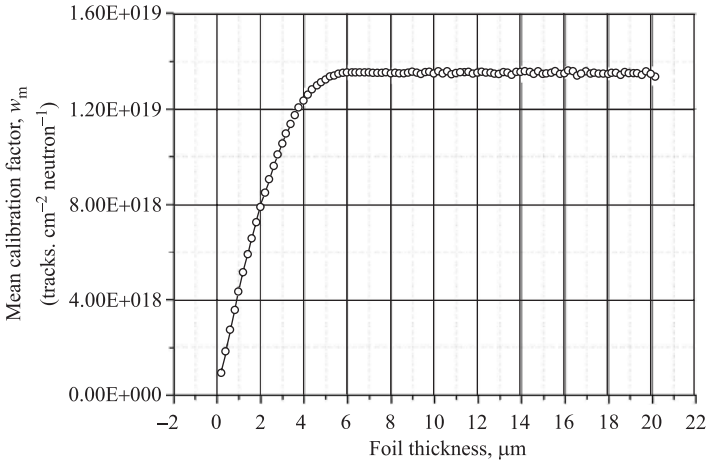

Fig. 2. Variations of the mean calibration factor $w_{\rm m}$ with fission foil thickness d. The calculations were made for the case of $\theta_c = 0$ and no track size restrictions are imposed

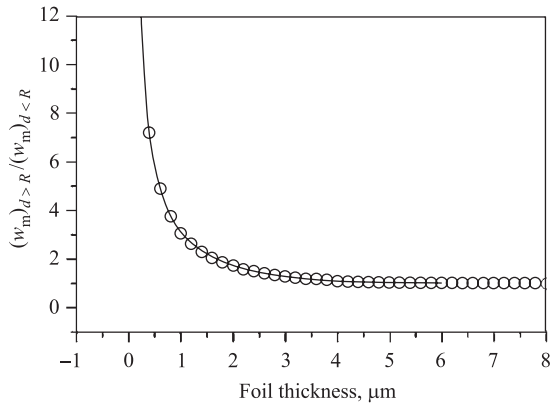

Fig. 3. Variations of the ratio of $w_{\rm m}$ at $d > R$ to that at $d < R$ as a function of the foil thickness d. Open circles refer to the MC results and the solid curve represents Eq. (7)

In the second integrity test of the MC code the ratio of w_{m} at $d > R$ to that at $d < R$, was calculated. From Eqs. (4) and (5) we expect this ratio to be equal to

$$\chi \equiv \frac{(w_{\mathrm{m}})_{d>R}}{(w_{\mathrm{m}})_{d<R}} = \frac{R}{2d\left(1 - \dfrac{d}{2R}\right)}. \tag{7}$$

Figure 3 illustrates the variation of the simulated and theoretical values of χ with the foil thickness. As can be seen, the MC results are in perfect agreement with the theory.

4.2. Estimation of Registration-Detection Efficiency. The overall detector efficiency (ratio of the number of etched tracks counted to the number of latent tracks that cross the detector surface) under a specific observation and detection condition can be expressed with the following relationship:

$$\varepsilon = \eta \cos^2 \theta_c, \tag{8}$$

where η represents fraction of the tracks that have been rejected by the observer (human or an automatic track counting system [14]) because of the limitations imposed by the

• track size;

• track density (at very high track densities the observer may underestimated the track density because of the overlapping track contours);

• observation conditions (such as contrast, brightness, density of background track-like objects, etc.).

4.2.1. Critical Angle Effect. For the detectors investigated in this work the θ_c values available in the literature were used (Table 3).

Table 3. The critical etching angle for different track detectors

Detector	θ_c	Ion type	Reference
Mica	4.5°		[15]
Lexan	2.5°		[15]
Macrofol	3°	^{252}Cf fission fragments	[15]
Soda glass	35.5°		[15]
Mica	4°		[16]
Lexan	3.5°	^{252}Cf fission fragments	[16]
Cellulose acetate	3°		[16]
Polycarbonate and polyethylene terephthalate	4°	U fission fragments	[17]
Soda glass	11.7 –17.4°	11.4 MeV/u ^{238}U ions	[18]

The fragments that enter the external detector have energies $E \leqslant E_{\mathrm{f}}$, where E_{f} is the undegraded energy of the fragments. The critical angle is energy-dependent [15], and the values given in Table 3 refer to the full energy fission

fragments and high energy ^{238}U ions. We discuss the influence of the ion energy on the θ_c separately for each type of detector used by us.

1) *Mica detectors*. For biotite mica detector the response curve of the track etch rate V_T as a function of primary ionization J [1] saturates at $J > 30$ (for K = 10.1) [19]. The track etch rate of the full energy fission fragments are on or about the saturation value of V_T. Examination of the primary ionization and total stopping power as a function of energy for fission-fragment-like ions in biotite and phlogopite micas indicates that for these detectors increase of the total kinetic energy of the fragments up to $\sim$ 1 GeV does not affect the track etch rate and therefore, θ_c remains almost constant. However, for low energy fission-fragment-like ions it is expected that V_T will decrease (and therefore θ_c will increase) with decreasing energy of the fragments. In the absence of saturation of the detector response, for fragments with energy higher than those of the ^{252}Cf fission, the θ_c will be less than $\theta_c = 4.5°$, and the use of this angle at higher energies can result almost in an error of 0.6% in the estimation of the w. On the other hand, at very low energies of fission fragments (the same order of stopping power as those of the alpha-recoils [20, 21]) for muscovite mica $V_T = 0.012 \cdot S_n$ μm/h and $V_\perp \approx 0.027\,\mu$m/h [22], where S_n represents the nuclear stopping power of the ion in units of GeV cm^{2}g^{-1} (samples have been etched in 40% HF at 25 °C). For $S_n \sim 10$ GeV cm^{2}g^{-1} corresponding to 100 keV median-heavy fragment one obtains $\theta_c = 13°$. As will be shown in the next section, a large number of tracks due to low energy fragments will be rejected because of track size restrictions, and as a consequence, in practice the effective θ_c for mica will never exceed $\sim$10°. Therefore, in muscovite mica, if θ_c for full energy fragments is used for energy degraded fragments, an error of almost 3% will be introduced in the calculated value of w.

2) *Lavsan detector*. Due to the very low value of θ_c for fission fragments in plastic detectors, the use of an unique θ_c value for full energy and energy-degraded fission fragments, will not introduce errors greater than those discussed in the case of the mica detectors.

3) *Soda glass detector.* For soda glass, the situation is rather different. The critical angle θ_c is strongly-dependent on the energy of fragments [15]. In this case, we calculated the weighted mean energy of the fragments entering into the external glass detector and then its corresponding $\theta_c = 44°$ was obtained from the data given by [15].

Therefore, in our calculations we used θ_c values of 4.5, 4 and 44° for mica, Lavsan and soda glass detectors, respectively.

4.2.2. Track Size Effect. For tracks that can be revealed by chemical etching, there are three options for estimating of the minimum detectable track size:

- minimum detectable track length, $L_{\min}$;
- minimum detectable projected track length, $(L_p)_{\min}$;
- minimum detectable track depth, δ.

Obviously, such a track size limitation is strongly-dependent on the means of observation and detection. The limits discussed in this paper refer to track analysis using an optical microscope with human operator.

On inspection of a sample under an optical microscope, the true track lengths are not directly available to the observer and therefore imposing a detection limit on the track length is not a realistic approach. Besides, when in MC calculations a track length limit of $L_{\min}$ is imposed as the track rejection criterion, all tracks with $L > L_{\min}$ are considered to be detectable. This cannot be true in practice because a track with $L > L_{\min}$ can have such a small depth (especially in detectors with a small θ_c such as mica) that its correct identification, and therefore counting is practically impossible.

Due to the fact that in track observation under an optical microscope the most obvious measurable parameter is the projected length, it seems that this is the best parameter to be considered as the track size limit. However, this is the most inappropriate of all the three mentioned above. The reason is that a minimum projected track length corresponds to very wide distributions of the track lengths and depths (due to the randomness of the dip angle θ). Such a choice automatically will reject all tracks with dip angles $\theta \geqslant \cos^{-1}[(L_p)_{\min}/R)]$, irrespective of their depth. Assuming that $(L_p)_{\min} = 2\mu$m [23] and $< R > \sim 10$ μm will exclude all tracks with $\theta \geqslant 75^\circ$ regardless of their etchable length and depth. Among the three above-mentioned size limit options the depth limit seems more suitable.

In order to understand the effects of imposition of a depth limit δ or a projected length limit $(L_p)_{\min}$, we determined the distributions of the length and depth of tracks that are rejected by each of these restrictions. To this end, for each track detector we first determined $(L_p)_{\min}$ and δ values at which $\kappa = \dfrac{|w_{\rm MC} - w_{\rm exp}|}{w_{\rm exp}} < 0.01$, where $w_{\rm MC}$ and $w_{\rm exp}$ are the MC and experimental values of the calibration factor, respectively. For each detector the MC code was run by setting θ_c equal to its corresponding value and then $(L_p)_{\min}$ or δ were varied in the interval from zero to 5 μm in steps of 0.01 μm, for $5{\cdot}10^5$ fission events per track size interval. In other words, the $(L_p)_{\min}$ or δ were treated as a fitting parameters. The mean values of the $(L_p)_{\min}$ or δ for which the condition $\kappa < 0.01$ was satisfied were used as the minimum detectable length or minimum detectable depth. For example, in the case of the artificial mica, the limits of $\langle(L_p)_{\min}\rangle = 1.69$ μm and $\langle\delta\rangle = 1.63$ μm were obtained.

Figure 4 shows the distributions of the rejected track length and depth when track size limits of $\langle(L_p)_{\min}\rangle = 1.69$ μm or $\langle\delta\rangle = 1.63$ μm were imposed. The presented results are for artificial mica in contact with a thick uranium foil.

From Fig. 4 it can be seen that the length distributions of the rejected tracks are very similar for the cases of the $(L_p)_{\min}$ and δ restrictions and whole number of the rejected tracks is $\sim 22\%$ of the total, in both cases. However, the depth

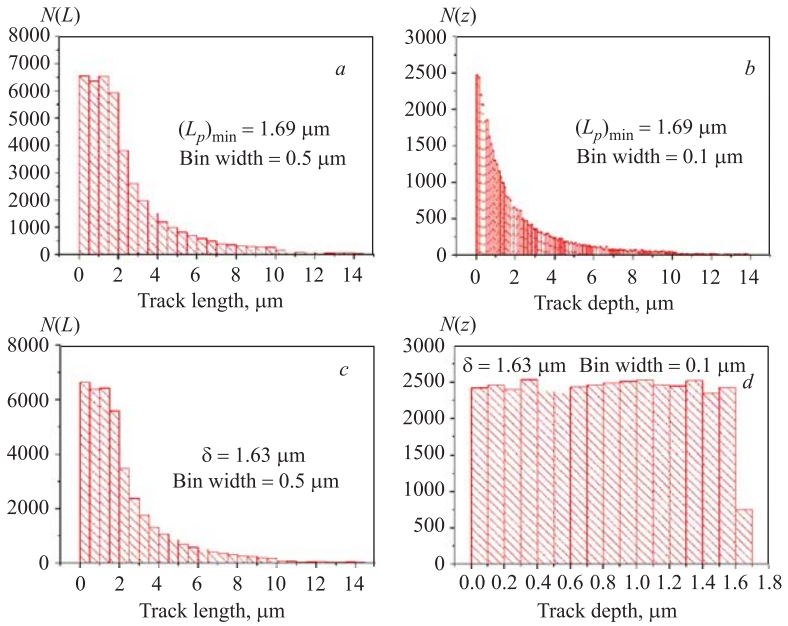

Fig. 4. Distribution of the rejected track length and depth in artificial mica when a projected track length limit $(L_p)_{\min}$ or track depth limit δ are imposed. a, b refer to the case when $\langle(L_p)_{\min}\rangle = 1.69$ μm, and c and d refer to the case of $\langle\delta\rangle = 1.63$ μm. The bin width for each histogram is given in the corresponding figure inset

distributions for these two cases are very different. When the $(L_p)_{\min}$ limit is imposed the rejected tracks are not necessarily those that may have been rejected in the track detection process (because tracks with adequate length and depth have been rejected). On the basis of these findings, we will use the mean track depth limit $\langle\delta\rangle$ as a measure of track delectability limit.

Table 4 gives the calculated $\langle\delta\rangle$ for different detectors. It seems that the values of the calculated $\langle\delta\rangle$ are rather high, compared to 0.8 μm suggested by [23]. But it must be remembered that this depth limit refers to an optical microscope with a human observer and includes observational as well as the track size restrictions expressed in terms of the track depth. Consistency between the $\langle\delta\rangle$ values obtained for different detectors suggests that experimental measurements have been made under similar conditions (the same observation tools and the same operator).

In track detectors, especially in minerals, there is a range deficit $\Delta R = R - R_e$ — the difference between the true range and etchable length of the ions

in the track detectors [24]. In our calculations, $\langle\delta\rangle$ indirectly includes both the required depth for track delectability as well as the effects of the range deficit that may exist.

Table 4. Comparison of the MC results and experiment whith the value of the calibration factor w for different track recording materials. The calculations are for randomly oriented fission tracks in thick natural uranium foil

Detector type	θ_c, deg	$\langle\delta\rangle$, μm	$\langle w_{\rm MC}\rangle$	$w_{\rm exp}$	Efficiency, $\varepsilon_{\rm MC}$
			Tracks, cm^{-2} · neutron^{-1}		
Natural mica	4.5	1.30	$(1.070 \pm 0.004)\cdot10^{19}$	$(1.07\pm0.04)\cdot10^{19}$	0.79
Artificial mica (Fluorophlogopite)	4.5	1.63	$(9.899 \pm 0.003)\cdot10^{18}$	$(9.9\pm0.03)\cdot10^{18}$	0.77
Lavsan plastic	4	1.22	$(1.179\pm 0.002)\cdot10^{19}$	$(1.18\pm0.04)\cdot10^{19}$	0.87
Soda glass	44*	1.79	$(5.886\pm 0.004)\cdot10^{18}$	$(5.9\pm0.02)\cdot10^{18}$	0.48

* See the text for details.

Also given in Table 4 the $w_{\rm MC}$, $w_{\rm exp}$ values (the same as those given in Table 2) and the overall detector efficiency $\varepsilon_{\rm MC}$ are calculated via the MC code. Alternatively, one can calculate the ε directly as $\varepsilon = \dfrac{w_{\rm exp}}{w_{\rm MC}(\delta=0,\theta_c=0)}$. Such efficiency values are valid only for observation conditions similar to those used in the calibration experiments.

4.3. Dependence of Calibration Factor on Angular Distribution of Fission Fragment. In this section, we calculate w for a thick foil and for the case when the angular distribution of the fission fragments is not isotropic. We assumed that at the moment of fission a linear momentum **p**, whose angle with the Z axis is β (Fig. 1), is transferred to the fission fragments. The final kinetic energy of the fragments includes the energy E_p associated with this momentum **p**. We calculated the $w_{\rm B}$ and $w_{\rm F}$ for three energy values of E_p = 0, 50 and 100 MeV as a function of the angle β. $E_p = 0$ represents the case when fission fragments are emitted isotropicaly.

In Fig. 5 variations of the $R_w = w_{\rm B}$ / $w_{\rm F}$ with β at three different values of the E_p are shown.

As can be seen and is expected for $\beta < 90°$, there are significantly larger numbers of tracks at the back surface of the foil compared to the front surface (see Fig. 1). At $\beta = 0°$ and $E_p = 100$ MeV the track density in the back detector is 22% higher than that in the front detector. Obviously, for $\beta > 90°$ inverse effect is expected. At $\beta = 90°$, $R_w = 1$ regardless of the magnitude of **p** and its associated energy E_p.

Figure 6 shows the variations of $w_{\rm m}$ with angle β for three different values of the E_p. It can be seen that $w_{\rm m}$ is independent of the magnitude of **p** and its associated energy E_p, as well as the angle of **p** with the Z axis.

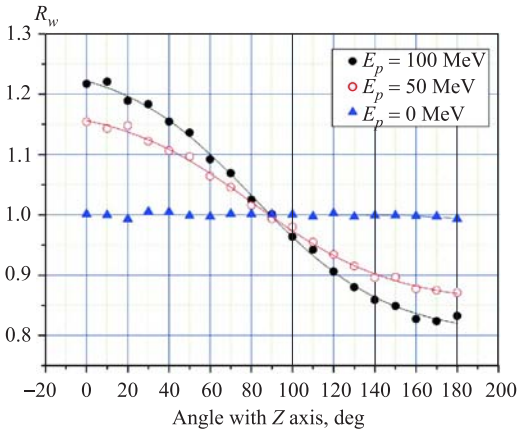

Fig. 5. The variations of the $R_w = w_{\mathrm{B}} / w_{\mathrm{F}}$ with β (see the text for details). Lines through the data points are to guide the eye

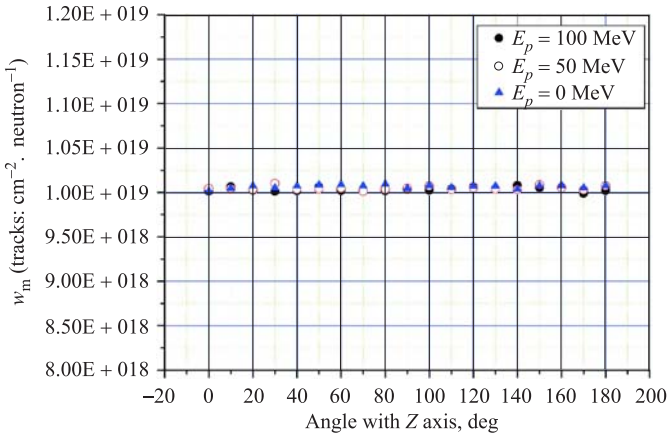

Fig. 6. The variations of w_{m} with angle β (see the text for details)

It must be noted that the angular distribution effects reported here are purely due to the reaction kinematics and these do not take into account the possible intrinsic angular distribution of the fragments in the frame of the fissioning nuclei which may depend on the mass asymmetry in the fission process and on the energy of the projectile [25]. Experimental results indicate that the anisotropy in the angular distribution of the fission fragments decreases with the increasing energy of the fission-inducing particles [25].

In order to have a complete understanding of the variation of w with incident particle (e. g. neutron) energy and orientation, detailed information on the fission

fragment angular distribution at high energy particle induced fission is required. Such information is not available at present, and further systematic experimental and theoretical research on this matter is required [26]. However, it seems that w_{m} will not be affected significantly with these findings.

4.4. Dependence of Calibration Factor on the Kinetic Energy of the Incident Particles. We used MCNPX 2.5e code [27] to calculate the recoil energy spectra in the interaction of energetic neutrons with ^{235}U nuclei. This code contains the current understanding of the fission process in the interaction of the energetic light nuclear particles with fissionable target nuclei. A ^{235}U foil of thickness 0.01 cm and diameter 1 cm was irradiated with orthogonally incident circular neutron beam of the same diameter as the target. We deliberately used a thin foil to minimize the possibility of interaction of the produced secondary particles with the target nuclei. Calculations were performed for neutron energies of 25, 100, 500, and 1000 MeV. The recoil energy spectra were obtained from the «HISTP» file generated by MCNPX 2.5e and by using the HTAPE code with edit option 16 [27, 28]. It must be noted that the final energy of the fragments also includes the possible kinetic energy of the fissioning nucleus, which may have gained in the course of all processes prior to fission.

Figure 7 shows the spectra of the total recoil energy at different incident neutron energies on ^{235}U foil. The data are presented in equal logarithmic energy binning.

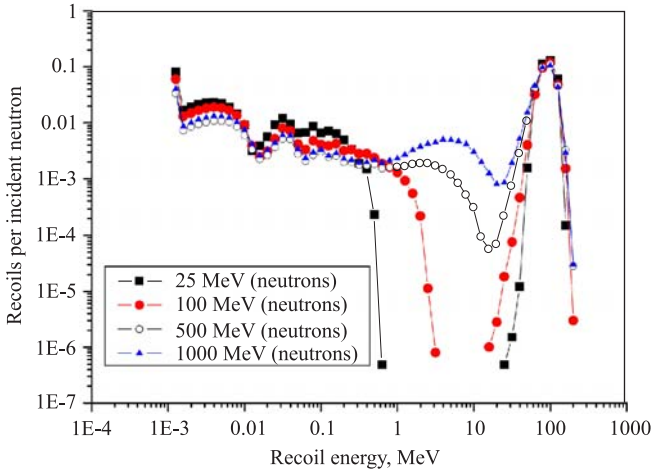

Fig. 7. Spectra of the total recoil energy deposited in a ^{235}U foil of thickness 0.01 cm at different incident neutron energies

The peak around 100 MeV is mainly due to the heavy and energetic recoiling nuclei (fragments). As can be seen, the variation of the incident neutron energy from 25 to 1000 MeV does not alter the position of the main peak.

The experimental evidence in support of the results of above calculations can be found in the early publications on the possible dependence of the fission fragment kinetic energy on incident particle energy [29–35]. These measurements have shown that although the fission fragment mass yield and distribution may be affected by the incident nucleon energy, the final kinetic energy of the fragments is dominated by the action of the Coulomb force between the fragments. In other words, the kinetic energy of the fragments does not vary noticeably with the excitation energy of the fissioning nucleus. As an example, the average total kinetic energy of the fission fragments in the interaction of 450 MeV protons with ^{238}U nuclei (163 $\pm$ 8 MeV) is essentially the same as that of ^{235}U by thermal neutrons or of 90 MeV neutron induced fission of ^{238}U [35].

In the interaction of high energy nucleons (e. g., $E > 100$ MeV) with target nuclei, at the moment of fission the residual fissioning nuclei will have varieties of charges, masses and excitation energies. Figure 8 illustrates the residual mass distributions in the fission of ^{238}U at different incident neutron energies (see the figure caption for details). As can be seen, the mass yield distribution changes dramatically with the incident neutron energy.

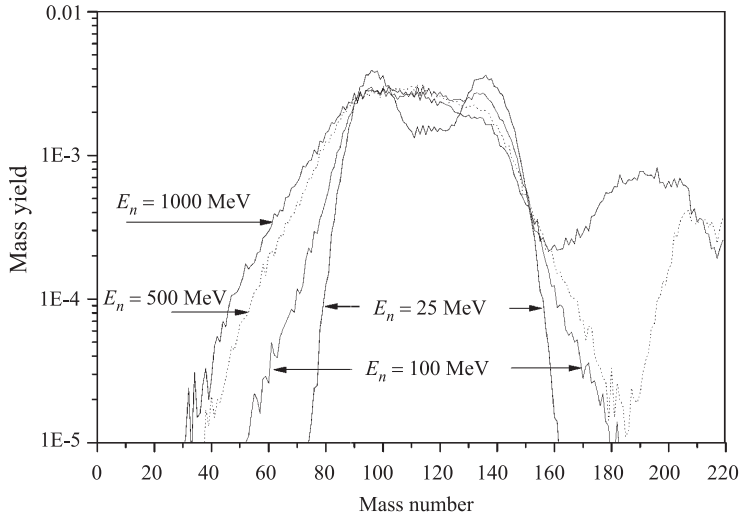

Fig. 8. Variations of the residual mass distribution in the fission of ^{238}U with incident neutron energy. The distributions were obtained via «HISTP» file generated by MCNPX 2.5e and by using the HTAPE code with edit option 8 [27, 28]. Only masses less than 220 are shown

Therefore, although the total average kinetic energy of the fission fragments can remain unchanged with energy of the incident particles, their mean range in matter can change due to variations in the fragment charge and mass compared to the case of low energy fission. But experimental results on the range of the fragments from high-energy fission of uranium show that the mean range in aluminium of fragments from ^{238}U fission induced by 18 MeV deuterons and 335 MeV protons are of the same order of magnitude as those reported for slow-neutron induced fission [10].

In the light of the above results and discussions, Eqs. (1)–(5) are also valid for the case of high-energy fission as far as the average total kinetic energy of the fragments and their average range in the matter are concerned.

5. CONCLUSIONS

The calibration factors w for determining of fission rate in fissionable materials were measured for mica, Lavsan, and soda glass track detectors. The neutron irradiations were carried out in standard thermal and 14.7 MeV neutron fields.

A Monte Carlo (MC) code was developed for detailed studies of w the results of which are in total agreement with theoretical expectations. It was found that the agreement between the experimental and MC results is achieved if a minimum track size limit for track detectability is imposed. It is shown that imposition of a track depth limit is more logical than track length or projected track length limits.

As the kinetic energy of the fission fragments is independent (or very weakly-dependent) on the fissioning nucleus's excitation energy, the energy of the bombarding particles does not affect the mean total kinetic energy of the fragments and their mean range in the matter. As a result, the calibration factor w will not be affected by the excitation energy of the fissioning nuclei as far as the range of the fragments in matter is concerned.

MC results illustrate that the mean value of w in the track detectors placed on both sides of a fission foil is independent of the angular distribution of the fragments.

Therefore, a w obtained by the irradiation of a fission foil-detector assembly (see Fig. 1) in a certain neutron field, can be used for determination of the fission rate in a particle (neutron) field of unknown characteristics (energy and angular distribution) if in the determination of w and in its subsequent use the mean value of the track densities in the track detectors on both sides of the fission foil is used.

The results of this paper will be used in the studies associated with accelerator driven systems and specifically in determination of fission-rate in the «Energy plus Transmutation» setup of the Joint Institute for Nuclear Research (JINR), Dubna, Russia [36].

Acknowledgements. The authors would like to thank staff of the F-1 reactor at the Russian Science Centre «Kurchatov Institute» (Moscow, Russia) and the Russian Special Primary Standard for Units at the «VNIIFTRI» Institute (Mendeleevo, Moscow Region, Russia) for providing the irradiation facilities for our samples.

Also we would like to thank Dr. J. J. Ulrichs for reading the manuscript and for many valuable comments.

REFERENCES

1. *Fleischer R. L., Price P. B., Walker R. M.* Nuclear Tracks in Solids. University of California Press, 1975.
2. *Malykhin A. P., Yaroshevich O. I., Levadni V. A., Roginetc L. P.* // Vestsi AS BSSR, Ser. Phys.-Energ. Nauk. 1970. V. 2. P. 16.
3. *Hashemi-Nezhad S. R., Brandt R., Westmeier W., Bamblevski V. P., Krivopustov M. I., Kulakov B. A., Sosnin A. N., Wan J.-S., Odoj R.* // Kerntechnik. 2001. V. 66. P. 47.
4. *Hashemi-Nezhad S. R., Brandt R., Westmeier W., Bamblevski V. P., Krivopustov M. I., Kulakov B. A., Sosnin A. N., Wan J.-S., Odoj R.* JINR, E1-2001-44. Dubna, 2001; Nucl. Instr. Meth. A. 2002. V. 482. P. 537.
5. Reactor Physics Constants. ANL-5800. Argonne National Laboratory, 1963. P. 667–681.
6. *Lemmel H. D.* Tech. Rep. No. 297. Vienna: IAEA, 1983. P. 71.
7. *Meadows J. W.* // Kernenergie. 1981. V. 24. P. 48.
8. *Meadows J. W.* // Ann. Nucl. Energy. 1988. V. 15. P. 421.
9. *Khan S., Forgue V.* // Phys. Rev. 1967. V. 163. P. 290.
10. *Douthett E. M., Templeton D. H.* // Phys. Rev. 1954. V. 94. P. 128.
11. http://t2.lanl.gov/cgi-bin/endf?1,458,/inet/WWW/data/data/ENDF-neutron/U/235e
12. http://t2.lanl.gov/cgi-bin/endf?1,458,/inet/WWW/data/data/ENDF-neutron/U/238e
13. *Ziegler J. F., Biersack J. P., Littmark U.* The Stopping and Range of Ions in Matter. Pergamon Press, 1985. See also www.SRIM.org. 1985.
14. *Dolleiser M., Hashemi-Nezhad S. R.* // Nucl. Instr. Meth. B. 2002. V. 198. P. 98.
15. *Khan H. A., Durrani S. A.* // Nucl. Instr. Meth. 1972. V. 98. P. 229.
16. *Dwivedi K. K.* // Radiat. Meas. 1997. V. 28. P. 149.

17. *Tretyakova S. P.* // Part. Nucl. 1992. V. 23. P. 364.

18. *Randhawa G. S., Virk H. S.* // Appl. Radiat. Isot. 1996. V. 47. P. 351.

19. *Hashemi-Nezhad S. R., Durrani S. A., Bull R. K., Green P. F.* // Nucl. Tracks Radiat. Meas. 1984. V. 8. P. 91.

20. *Huang W. H., Walker R. M.* // Science. 1967. V. 155. P. 1103.

21. *Hashemi-Nezhad S. R., Durrani S. A.* // Nucl. Tracks. 1981. V. 5. P. 189.

22. *Price P. B., Salamon M. H.* // Phys. Rev. Lett. 1986. V. 56. P. 1226.

23. *Jonckheere R., Haute P. V.* // Radiat. Meas. 2002. V. 35. P. 29.

24. *Fleischer R. L., Price P. B., Symes E. M., Miller D. S.* // Science. 1964. V. 143. P. 349.

25. *Meadows J. W.* // Phys. Rev. 1958. V. 110. P. 1109.

26. *Prokofiev A. et al.* // Proc. of the Int. Conf. on Nuclear Data for Science and Technology, Santa Fe, USA, September 26–October 1, 2004. V. 769. P. 800–803.

27. *Hendricks J. S. et al.* MCNPX, VERSION 2.5.e. Report No. LA-UR-04-0569. Los Alamos National Laboratory, 2004.

28. *Prael R. E., Lichtenstein H.* User Guide to LCS: The LAHET Code System. Report No. LA-UR-89-3014. Los Alamos National Laboratory, 1989.

29. *Wahl J. S.* // Phys. Rev. 1954. V. 95. P. 126.

30. *Jungerman J. J., Wright S. C.* // Phys. Rev. 1949. V. 76. P. 1112.

31. *Friedland S. S.* // Phys. Rev. 1951. V. 84. P. 75.

32. *Fowler J. L., Rosen L.* // Phys. Rev. 1947. V. 72. P. 926.

33. *Brunton D. C., Hanna G. C.* // Phys. Rev. 1949. V. 75. P. 990.

34. *Baranov I. A., Protopopov A. N., Eismont V. P.* // Atom. En. 1962. V. 12. P. 150.

35. *Sugarman N., Münzel H., Panontin J. A., Wielgoz K., Ramaniah M. V., Lange G., Lopez-Mencheropp E.* // Phys. Rev. 1966. V. 143. P. 952.

36. *Krivopustov M. I. et al.* // Kerntechnik. 2003. V. 68. P. 48–54; JINR Preprint E1-2004-79. Dubna, 2004.

Received on April 19, 2006.

Корректор *Т. Е. Попеко*

Подписано в печать 24.07.2006.
Формат 60 × 90/16. Бумага офсетная. Печать офсетная.
Усл. печ. л. 1,43. Уч.-изд. л. 2,05. Тираж 365 экз. Заказ № 55417.

Издательский отдел Объединенного института ядерных исследований
141980, г. Дубна, Московская обл., ул. Жолио-Кюри, 6.
E-mail: publish@pds.jinr.ru
www.jinr.ru/publish/